SPIN-ORBIT SECONDARY RESONANCE DYNAMICS OF ENCELADUS

J. WISDOM
Department of Earth, Atmospheric, and Planetary Sciences, Massachusetts Institute of Technology,
77 Massachusetts Avenue, Cambridge, MA 02139; wisdom@poincare.mit.edu

ABSTRACT

For Enceladus the frequency of small-amplitude oscillations about the synchronous rotation state is approximately one-third the orbital frequency. Near this commensurability a period-three bifurcation occurs; on a surface of section a period-three chain of secondary islands appears near the synchronous island center. Forced libration in this resonance may be large and would imply large tidal heating. This paper explores the possibility that Enceladus is or once was locked in this period-three librational resonance, and that the observed resurfacing of Enceladus is a consequence.

Key words: celestial mechanics — gravitation — methods: analytical — methods: numerical —
planets and satellites: individual (Enceladus, Mimas, Saturn) — planets and satellites: formation

1. INTRODUCTION

Enceladus, now there's a puzzle. A substantial portion of the imaged surface of Enceladus is covered by smooth plains that are nearly crater-free. From the crater density, these plains are estimated to be less than a billion years old, perhaps less than 100 million years old. Thus, much of the surface of Enceladus has been resurfaced. There may be two distinct smooth plains regions, one of which is lightly cratered. So, Enceladus may have been resurfaced more than once. The only viable source of energy for this activity on Enceladus is tidal heating, but the estimated rate of tidal heating is not only too small to initiate melting in Enceladus but probably too small even to maintain a molten layer produced at some earlier epoch (for which one would still need to identify an adequate heat source for the initial formation). There are many discussions of the problem (Squyres et al. 1983; Schubert et al. 1986; Morrison et al. 1986; Squyres & Croft 1986; Peale 2003). A successful explanation must pass the "Mimas test": Squyres et al. (1983) pointed out that Mimas is comparable in size to Enceladus, has a larger orbital eccentricity, and is closer to Saturn, so tidal heating in Mimas should be substantially larger (about a factor of 25) than heating in Enceladus, yet Mimas does not show evidence of tidal heating.

Squyres et al. (1983) suggested that Enceladus may have more ammonia than Mimas. Not only does adding ammonia lower the melting temperature (and so lower the heating required for resurfacing), but an ammonia-water solution with greater than 20% mole fraction of ammonia (perhaps achieved as ice freezes out) is less dense than ice and so might spew out onto the surface, perhaps even creating the E ring. But ammonia has not been detected on the surface.

Lissauer et al. (1984) proposed that Enceladus was recently locked in an orbital resonance with Janus, which was disrupted in the last 10 million years by an impact or when Enceladus became locked in the current Enceladus-Dione resonance. If locked in this resonance with Janus, Enceladus would have had a larger forced eccentricity and thus been subject to larger tidal heating. But in their model the eccentricity only reaches values near 0.01, compared with the present 0.0045, so the rate of tidal heating is only enhanced by a factor of about 5. Thus, their

scenario does not pass the Mimas test. There are also numerous questionable aspects of the dynamics.

Ross & Schubert (1989) found that estimates of tidal heating with a viscoelastic Maxwell rheology can be substantially larger than for Darwin models with a bulk effective tidal Q. They considered both homogeneous ice models and models with a liquid ammonia-water decoupling layer. They argue that their models give sufficient heating to explain the observed activity on Enceladus. Ross & Schubert do not discuss why their models do not also predict substantial tidal heating of Mimas. If a homogeneous ice model predicts substantial tidal heating of Enceladus, should not this also be the case for Mimas?

The dichotomy between Enceladus and Mimas suggests that some additional heating mechanism is operating on Enceladus and that this heating mechanism results from some characteristic that Enceladus possesses that other satellites do not share. One characteristic that is unique to Enceladus is that the frequency of small-amplitude oscillations about synchronous rotation is nearly commensurate with its orbital frequency: specifically, the frequency of small-amplitude oscillations for Enceladus is approximately one-third its orbital frequency.

In their analysis of *Voyager* images of Enceladus, Dermott & Thomas (1994) found that the shape of Enceladus was well represented by a triaxial ellipsoid with principal radii $a = 256.3 \pm 0.3$ km, $b = 247.3 \pm 0.3$ km, and $c = 244.6 \pm 0.3$ km. They interpret this figure in terms of hydrostatic models and deduce that Enceladus has a density below 1.12 g cm^{-3}, with a preferred value near 1.00 g cm^{-3}. The ratio of moments of inertia determines the spin-orbit libration frequency. Assuming uniform density, the implied $(B - A)/C$ is 0.03573 ± 0.0017. More to the point, the implied ratio of the librational frequency to the orbital frequency is $\epsilon = [3(B - A)/C]^{1/2} = 0.3274 \pm 0.0077$. The error is purely formal; the real error is probably larger.

This near commensurability has very interesting dynamical consequences. For ϵ near $\frac{1}{3}$ there is period-three bifurcation in the spin-orbit phase space. On a surface of section, a chain of three secondary islands appears near the center of the synchronous island. Now, if Enceladus is locked in this period-three island, then there is a forced libration of the figure of

Enceladus relative to Saturn. Depending on the system parameters, the rate of tidal heating due to this forced secondary resonance libration can be enhanced by a factor of 100 to 1000 over the rate of tidal heating without secondary resonance libration.

A number of natural satellites are significantly out of round, with ϵ larger than $\frac{1}{3}$. For instance, Dermott & Thomas (1988) measured the elliptical radii for Mimas. From these, ϵ for Mimas is estimated to be near 0.44. Such satellites also display secondary resonances on their surfaces of section, but because ϵ is not near a low-order commensurability, these secondary islands are not near the synchronous island center and so are unlikely to play any role in the dynamics of these satellites.

This paper examines the dynamics of the $3:1$ secondary spin-orbit resonance, computes the consequent rate of tidal heating, and discusses mechanisms that might have placed Enceladus into this unique dynamical state.

2. SPIN-ORBIT DYNAMICS

The Hamiltonian governing the rotational dynamics of an out-of-round satellite in a fixed elliptical orbit with the spin axis perpendicular to the orbit plane is

$$H(t, \theta, p) = \frac{p^2}{2C} - \frac{\epsilon^2 n^2 C}{4} \left[\frac{a}{r(t)} \right]^3 \cos 2[\theta - f(t)] \qquad (1)$$

(Wisdom et al. 1984; Wisdom 1987; Sussman & Wisdom 2001), where

$$\epsilon = \sqrt{3(B - A)/C}. \qquad (2)$$

The moments of inertia are $A < B < C$, n is the orbital frequency, θ measures the orientation of the axis of minimum moment from the line to pericenter, p is the angular momentum conjugate to θ, a is the semimajor axis of the orbit, r is the planet-to-satellite distance, and f is the true anomaly (the angle from the pericenter to the satellite).

For nonzero eccentricity, the spin-orbit problem exhibits the full suite of phenomena generally found in nonlinear Hamiltonian systems, such as nonlinear resonances and chaos. For small eccentricity, the phase space is dominated by the synchronous resonance in which the angle $\phi = \theta - nt$ oscillates about 0 or π. There is a chaotic zone surrounding the synchronous resonance. Other primary resonances are present, the two largest are the $3:2$ and $1:2$, in which the body rotates three or one times, respectively, for every two orbits. Mercury is in the $3:2$ resonance. A surface of section is generated by plotting the rate of change of the orientation ($\dot{\theta}$) versus the orientation (θ) at each pericenter for a number of orbits for a representative set of initial conditions. A typical surface of section for parameters appropriate for Enceladus is shown in Figure 1. The distinctive feature of the surface of section for Enceladus is the period-three chain of islands near each of the synchronous island centers.

3. SPIN-ORBIT SECONDARY RESONANCES

Here we develop an approximate model for the $3:1$ secondary resonances for synchronous rotation in the spin-orbit problem. We use standard techniques of Hamiltonian perturbation theory (Sussman & Wisdom 2001).
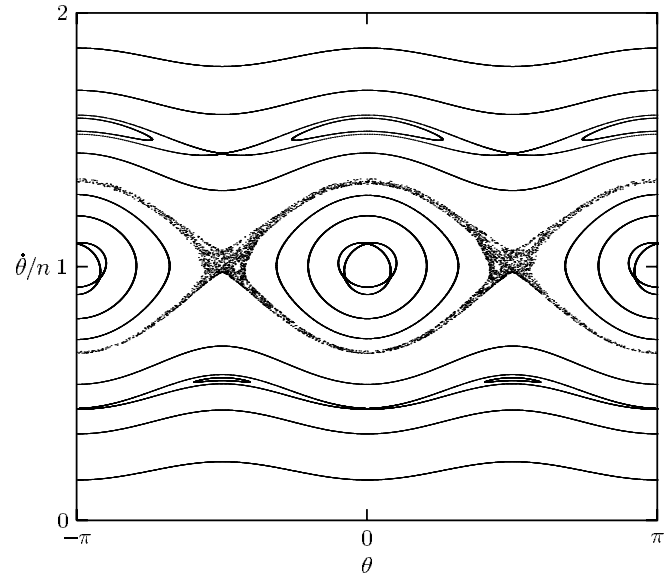

FIG. 1.—A surface of section for $\epsilon = 0.34$ and $e = 0.0045$. The dominant feature is the synchronous island. The $3:2$ and $1:2$ resonances are above and below the synchronous island, respectively. The synchronous island is surrounded by a small chaotic zone. Near each of the synchronous equilibria there is a chain of three islands, in which the libration about synchronous rotation is in a $3:1$ resonance with the orbital motion.

For a fixed orbit the planet-to-satellite distance and the true anomaly are periodic. Expanding these as Fourier series, the spin-orbit Hamiltonian is

$$H(t, \theta, p) = \frac{p^2}{2C} - \frac{\epsilon^2 n^2 C}{4} \sum_k \mathcal{H}_k(e) \cos(2\theta - knt) \qquad (3)$$

with coefficients $\mathcal{H}_2(e) = 1 - 5e^2/2$, $\mathcal{H}_3(e) = 7e/2$, and $\mathcal{H}_1(e) = -e/2$, to second order in e.

We consider the terms that depend on the eccentricity as a perturbation and write

$$H = H_0 + H_1, \qquad (4)$$

where

$$H_0(t, \theta, p) = \frac{p^2}{2C} - \frac{\epsilon^2 n^2 C}{4} \cos(2\theta - 2nt), \qquad (5)$$

$$H_1(t, \theta, p) = -\frac{\epsilon^2 n^2 C}{4} \left[\frac{7e}{2} \cos(2\theta - 3nt) - \frac{e}{2} \cos(2\theta - nt) \right], \qquad (6)$$

keeping only the terms linear in e.

The Hamiltonian H_0 is solvable. First make a canonical transformation to a rotating frame $\phi = \theta - nt$, with conjugate momentum $\Phi = p - nC$. The new Hamiltonian is

$$H_0'(t, \phi, \Phi) = \frac{\Phi^2}{2C} - \frac{\epsilon^2 n^2 C}{4} \cos 2\phi. \qquad (7)$$

This is time-independent and has a single degree of freedom, and so the solution is reducible to quadratures. The solutions

can be expressed in terms of elliptic functions. The perturbation is also transformed:

$$H_1'(t, \phi, \Phi) = -\frac{\epsilon^2 n^2 C}{4}\left[\frac{7e}{2}\cos(2\phi - nt) - \frac{e}{2}\cos(2\phi + nt)\right].$$
(8)

With the goal of approximating the secondary resonances between the frequency of oscillation and the orbital frequency, we next make the transformation to action-angle coordinates for the Hamiltonian (eq. [7]) in the oscillation region. The action J is the area on the phase plane (ϕ, Φ), divided by 2π. The conjugate angle ψ evolves linearly in time. The transformed Hamiltonian depends only on the action:

$$H_0''(t, \psi, J) = \frac{1}{4}\epsilon^2 n^2 C\left(-1 + \tilde{J} - \frac{1}{16}\tilde{J}^2 - \frac{1}{256}\tilde{J}^3 + \cdots\right)$$
$$= -\frac{1}{4}\epsilon^2 n^2 C + \epsilon n J - \frac{1}{4C}J^2 - \frac{1}{16\epsilon n C^2}J^3 + \cdots,$$
(9)

where $\tilde{J} = (4/\epsilon)(J/nC)$. Note that for small J the frequency, the coefficient of the linear term in J, is just ϵn, as expected. The relation between the action-angle coordinates (ψ, J) and ϕ is

$$2\phi = \left(2\tilde{J} + \frac{1}{4}\tilde{J}^2 + \frac{27}{512}\tilde{J}^3 + \cdots\right)^{1/2}\sin\psi$$
$$+ \frac{1}{192}\left[(2\tilde{J})^3\left(1 + \frac{9}{16}\tilde{J} + \cdots\right)\right]^{1/2}\sin 3\psi + \cdots. \quad (10)$$

Compare these expressions with those for a harmonic (small ϕ) approximation to the Hamiltonian in equation (7):

$$H_0'(t, \phi, \Phi) \approx \frac{\Phi^2}{2C} + \frac{\epsilon^2 n^2 C\phi^2}{2}.$$
(11)

The canonical transformation to action-angle coordinates is

$$\phi = (2J/\alpha)^{1/2}\sin\psi, \quad \Phi = (2J\alpha)^{1/2}\cos\psi, \quad (12)$$

where $\alpha = \epsilon nC$. The transformed Hamiltonian is

$$H_0'(t, \phi, \Phi) \approx \epsilon n J,$$
(13)

which again gives ϵn for the frequency of small-amplitude oscillations. Notice that in this approximation the expression for the angle ϕ agrees with the first term of the full expression, equation (10).

Next we write the perturbation in terms of the full action-angle coordinates. For small ϕ it is appropriate to write the ϕ dependence of H_1' as a series,

$$H_1'(t, \phi, \Phi) = -\tfrac{1}{4}\epsilon^2 n^2 C(3eC_2\cos nt + 4eS_2\sin nt) \quad (14)$$

with

$$C_2 = \cos 2\phi = 1 - \tfrac{1}{2}(2\phi)^2 + \cdots$$
$$S_2 = \sin 2\phi = 2\phi - \tfrac{1}{6}(2\phi)^3 + \cdots. \quad (15)$$

The expression for 2ϕ is of the form

$$2\phi = F_1\sin\psi + F_3\sin 3\psi + \cdots, \quad (16)$$

where

$$F_1 = \sqrt{2\tilde{J}} + \frac{1}{16}(\sqrt{2\tilde{J}})^3 + \cdots,$$
$$F_3 = \frac{1}{192}(\sqrt{2\tilde{J}})^3 + \cdots. \quad (17)$$

Making these substitutions in equation (14), writing the result as a Poisson series in ψ and nt, and then picking out the terms with argument $3\psi - nt$, which are slow near the 3:1 secondary resonance, the resonant part of the perturbation is

$$H_{3:1}''(t, \psi, J)$$
$$= -\frac{1}{4}\epsilon^2 n^2 Ce\left(\frac{1}{12}F_1^3 + 2F_3 + \cdots\right)\cos(3\psi - nt)$$
$$= -\frac{1}{4}\epsilon^2 n^2 Ce\frac{3}{32}(\sqrt{2\tilde{J}})^3\cos(3\psi - nt). \quad (18)$$

We have kept only the leading term. Without the F_3 contribution, the coefficient is $1/12$ rather than $3/32$.

Keeping terms up to J^2 and dropping the constant term, the full 3:1 secondary resonance Hamiltonian is

$$H_{3:1}(t, \psi, J) = \epsilon n J - \frac{1}{4C}J^2 - e\frac{3}{16}\left(\frac{n\epsilon}{C}\right)^{1/2}$$
$$\times (\sqrt{2J})^3\cos(3\psi - nt). \quad (19)$$

Finally, we make a canonical transformation to the resonance variable $\psi' = \psi - nt/3$, with conjugate momentum $J' = J$. The resonance Hamiltonian is

$$H_{3:1}'(t, \psi', J') = n^2 C[\delta\hat{J} - \tfrac{1}{4}\hat{J}^2 - \gamma(\sqrt{2\hat{J}})^3\cos 3\psi'], \quad (20)$$

where $\hat{J} = J'/(nC)$, $\delta = \epsilon - \frac{1}{3}$, and $\gamma = (3/16)e\sqrt{\epsilon}$. Apart from the factor $n^2 C$, the resonance Hamiltonian is written in terms of dimensionless quantities, $\hat{J}$ is the dimensionless action, δ is a parameter that determines how close the system is to resonance, and γ measures the strength of the resonance. The resonance trajectories are contours of this time-independent, one-degree-of-freedom Hamiltonian. Trajectories of the resonance model are compared with the surface of section in Figure 2.

As δ is varied, there are special points where the phase portrait changes qualitatively. We can find these by solving for the equilibrium points. The equilibrium points have a threefold symmetry, with one set along the axis for which $\sin\psi' = 0$. In the variables $x = (2\hat{J})^{1/2}\cos\psi'$, $y = (2\hat{J})^{1/2}\sin\psi'$, the equilibria for $y = 0$ satisfy the equation

$$0 = (x^2/4 + 3\gamma x - \delta)x. \quad (21)$$

So, the origin is always an equilibrium and the other equilibria are solutions of a quadratic equation. For $9\gamma^2 + \delta > 0$, there are two nonzero solutions. In terms of ϵ this bifurcation point is

$$\epsilon_1 = \frac{1/3}{1 + (9/16)^2 e^2}. \quad (22)$$

The second special point is where one of the nonzero roots passes through zero. This occurs for $\delta = 0$, or $\epsilon_2 = \frac{1}{3}$. In the phase plane the bifurcation pattern is as follows: For $\epsilon < \epsilon_1$ there is a single equilibrium point. As ϵ is increased to ϵ_1, a
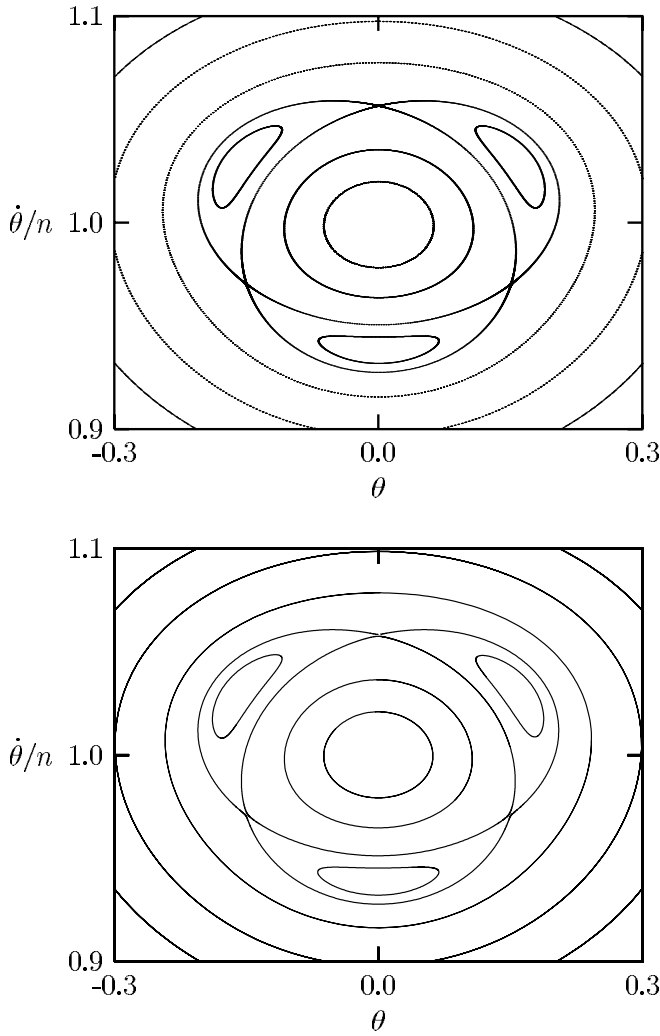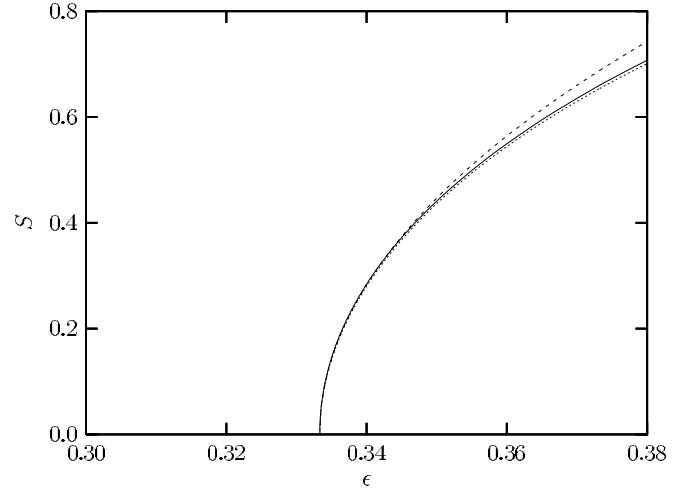
Fig. 3.—Amplitude of secondary libration (in radians) at the stable 3:1 fixed point in the full spin-orbit problem (*solid curve*), compared with the estimated amplitude using perturbation theory. The dashed curve uses both terms in eq. (24); the dotted curve uses just the first.

Fig. 2.—*Top*, surface of section for $\epsilon = 0.336$ and $e = 0.0045$, showing the 3:1 secondary islands; *bottom*, plot showing trajectories of the perturbative resonance Hamiltonian, on the surface of section. The agreement of the perturbative model with the surface of section is good.

cusp appears at a finite distance away from the origin, from which a stable and unstable point emerge for larger ϵ. The cusp appears at $x_1 = -3\gamma/2$, $y_1 = 0$. The equilibrium farther from the origin is stable. As δ is increased to zero, the unstable point goes through zero. As δ (and ϵ) is increased further, the stable and unstable equilibria move away from the origin. The action of the stable equilibrium is

$$\sqrt{2\hat{J}} = 6\gamma + 2(9\gamma^2 + \delta)^{1/2}. \qquad (23)$$

For parameters relevant to Enceladus, the dependence on γ is weak, and to a good approximation, at the stable equilibrium $(2\hat{J})^{1/2} = 2\sqrt{\delta}$. The corresponding amplitude of libration can be determined using equation (10). The amplitude is approximately

$$S = \tfrac{1}{2}(2\tilde{J} + \tfrac{1}{4}\tilde{J}^2)^{1/2}. \qquad (24)$$

Figure 3 compares the perturbative estimate of the amplitude of libration at the stable fixed point with the actual amplitude of libration (determined numerically). The agreement is good,

particularly near the point of bifurcation. The truncated estimate is better than the more complete estimate.

4. TIDAL HEATING

Time-dependent tidal distortion of a body leads to internal heating. For a synchronously rotating body in an eccentric orbit, the rate of energy dissipation is

$$\frac{dE}{dt} = \frac{21}{2}\frac{k_s f}{Q_s}\frac{Gm_p^2 nR_s^5 e^2}{a^6} \qquad (25)$$

(Peale & Cassen 1978; Peale et al. 1979; Peale 1999), where k_s is the satellite potential Love number, Q_s is the satellite effective tidal Q, $f > 1$ is an enhancement factor to account for a partially molten interior, G is the gravitational constant, a is the orbit semimajor axis, m_p is the mass of the host planet, n is the orbital mean motion (and rotation rate), which is approximately $(Gm_p/a^3)^{1/2}$, R_s is the satellite radius, and e is the orbital eccentricity. The derivation of this formula assumes that the body is incompressible, the rotation is uniform and synchronous, and the body is small enough that the displacement Love number h_s is $5k_s/3$. We may view this dissipation as arising from two distinct sources of time dependence in the tide: time variation in the distance to the tide-raising planet, and the optical libration (the relative rocking motion of a uniformly rotating satellite relative to the planet that results from the nonuniform motion in the elliptic orbit). Here this formula is rederived and generalized to include obliquity, forced libration, and forced secondary libration.

Let U_T be the tide-raising potential. The satellite may be thought of as consisting of a myriad of small constituent mass elements. The force on each mass element is the negative gradient of the potential energy, where the potential energy is the tidal potential multiplied by the mass of the constituent. The rate at which work is done on each constituent is the scalar product of this force with the velocity of the constituent. Integrating over the volume of the satellite gives the rate at which work is done on the satellite:

$$\frac{dE}{dt} = -\int_{\text{body}} \rho \boldsymbol{v} \cdot \boldsymbol{\nabla} U_T \, dV, \qquad (26)$$

where ρ is the density and dV is the volume element. To a good approximation the satellite may be assumed to be incompressible, $\boldsymbol{\nabla} \cdot \boldsymbol{v} = 0$ (Peale & Cassen 1978). The chain rule gives

$$\boldsymbol{\nabla} \cdot (U_T \boldsymbol{v}) = \boldsymbol{v} \cdot \boldsymbol{\nabla} U_T + U_T \boldsymbol{\nabla} \cdot \boldsymbol{v}, \tag{27}$$

so with the assumption of incompressibility, the rate of energy dissipation is

$$\frac{dE}{dt} = -\int_{\text{body}} \rho \boldsymbol{\nabla} \cdot (U_T \boldsymbol{v}) dV. \tag{28}$$

If we ignore any variation of density in the body, Gauss's theorem allows us to write the rate of energy dissipation as a surface integral,

$$\frac{dE}{dt} = -\rho \int_{\text{surface}} U_T \boldsymbol{v} \cdot \boldsymbol{n} \, dS, \tag{29}$$

where $\boldsymbol{n}$ is the normal to the surface and dS is the surface area element. Now, $\boldsymbol{v} \cdot \boldsymbol{n}$ is the rate at which the height of the surface changes. The height of the tide at any point on the surface is approximately

$$\Delta r = -h_s U_T'/g, \tag{30}$$

where h_s is the displacement Love number for the satellite, g is the local acceleration of gravity, and the prime on U_T indicates that the tidal potential is given a phase delay because the dissipative tidal response lags the forcing. So,

$$\frac{dE}{dt} = -\frac{\rho h_s}{g} \int_{\text{surface}} U_T \frac{d}{dt}(U_T') dS. \tag{31}$$

The tide-raising gravity gradient potential is

$$U_T = -\frac{Gm_p R^2}{r^3} P_2(\cos \alpha), \tag{32}$$

where P_2 is the second Legendre polynomial, α is the angle at the center of the satellite between the planet-to-satellite line and the point in the satellite where the potential is being evaluated, R is the distance from the satellite center to the evaluation point, and r is the planet-to-satellite distance.

Consider motion in a fixed elliptical orbit, with small eccentricity e. Choosing rectangular coordinates with the x-axis aligned with the orbit pericenter and the orbit in the (x, y)-plane, the orbital position is

$$\boldsymbol{o} = (r \cos f, r \sin f, 0) \tag{33}$$

with true anomaly f. For small eccentricity,

$$r^{-1} = a^{-1}(1 + e \cos nt),$$

$$\cos f = \cos nt + e(\cos 2nt - 1),$$

$$\sin f = \sin nt + e \sin 2nt, \tag{34}$$

all to first order in e. These expressions are easily generalized to higher order in eccentricity. In terms of the planetocentric longitude λ and colatitude θ, the rectangular components of

a surface element in the unrotated satellite (or at the initial time) are

$$\boldsymbol{s}_0 = (R \sin \theta \cos \lambda, R \sin \theta \sin \lambda, R \cos \theta). \tag{35}$$

Assuming uniform synchronous rotation about the z-axis (perpendicular to the orbit plane), the rectangular components of this element at time t are

$$\begin{aligned}\boldsymbol{s} &= \mathbf{R}_z(nt)\boldsymbol{s}_0 \\ &= (R \sin \theta \cos (\lambda + nt), R \sin \theta \sin (\lambda + nt), R \cos \theta),\end{aligned} \tag{36}$$

where $\mathbf{R}_z(\theta)$ is an active rotation about the z-axis by the angle θ. The scalar product of the surface element with the orbital position gives $\boldsymbol{o} \cdot \boldsymbol{s} = rR \cos \alpha$. This completes the expression for the tidal potential as a function of time and location on the surface. The delayed tidal potential U_T' is found by replacing nt by $nt + \Delta$ in the expression for U_T.

The average rate of energy dissipation is found by carrying out the surface integral, equation (31), and averaging over an orbital period. These integrals are straightforward and will not be shown. The result is

$$\frac{dE}{dt} = -\frac{21}{2}\frac{3h_s}{5}\frac{Gm_p^2 R_s^5 ne^2}{a^6} \sin \Delta. \tag{37}$$

The contribution due to the optical libration can be separated from that due to radial variation. Of the factor 21/2, 9/2 can be attributed to the radial variation, and 12/2 to the optical libration. The optical libration is more important by a factor of 4/3.

For small homogeneous spherical elastic bodies, the Love numbers are approximately given by

$$h_s = \frac{5/2}{1 + 19\mu/(2\rho gR)} \approx \frac{5\rho gR}{19\mu} \tag{38}$$

(Thompson 1863; Love 1944) and $k_s = \frac{3}{5}h_s$, where μ is the rigidity. The latter approximation is for the case where the rigidity is large (compared with ρgR). This formula and the relationship between k_s and h_s are not valid for inhomogeneous bodies, such as planetary bodies for which the density varies with radius. Estimates of k_2 and h_2 for the Moon from lunar laser ranging (Williams et al. 2003) are $k_2 = 0.0257 \pm 0.0025$ and $h_2 = 0.029 \pm 0.013$. These are nominally inconsistent with the $5:3$ ratio expected for a small homogeneous body, but barely consistent given the large estimated error in h_2. Nevertheless, assuming $k_s = 3h_s/5$, replacing $\sin \Delta$ by $-1/Q_s$, and adding the enhancement factor f, we have derived equation (25). Using the approximation to equation (38) for large rigidity, the rate of tidal heating becomes

$$\frac{dE}{dt} = \frac{42}{19}\frac{\pi \rho^2 R^7 n^5 e^2}{\mu Q}, \tag{39}$$

in agreement with the corrected expression in Peale (2003).

Next we assume the rotation is locked to the center of a threefold secondary resonance. To lowest order in the libration amplitude S, the location of the surface element is now (generalizing eq. [36])

$$\boldsymbol{s}' = \mathbf{R}_z(nt - S \sin (nt/3))\boldsymbol{s}_0. \tag{40}$$

For small S, we may expand

$$s' = s + SR(\sin \theta \sin (\lambda + nt) \sin (nt/3),$$
$$- \sin \theta \cos (\lambda + nt) \sin (nt/3), 0). \quad (41)$$

The rest of the calculation proceeds as before. We assume the tidal response is delayed by replacing nt by $nt + \Delta$. In this case, the averaging is over three orbital periods, to complete a secondary cycle, instead of one.

For completeness we include two other sources of tidal dissipation: the forced libration and satellite obliquity. To add the forced libration, we take

$$s' = \mathbf{R}_z(nt - F \sin nt - S \sin (nt/3))s_0. \quad (42)$$

The amplitude of the forced libration is approximately

$$F = \frac{2e\epsilon^2}{1 - \epsilon^2} \quad (43)$$

(Wisdom et al. 1984). And then, with obliquity I the expression for the surface element is

$$s' = \mathbf{R}_z(\Omega)\mathbf{R}_x(I)\mathbf{R}_z(nt - F \sin nt - S \sin (nt/3))s_0, \quad (44)$$

where Ω is the ascending node of the equator relative to the pericenter.

The generalization of equation (25) is found to be

$$\frac{dE}{dt} = \left[\frac{9}{2}e^2 + \frac{3}{2}(2e + F)^2 + \frac{1}{2}S^2 + \frac{3}{2}(\sin I)^2 \right]$$
$$\times \frac{3h_s}{5} \frac{1}{Q_s} \frac{f Gm_p^2 nR_s^5}{a^6}. \quad (45)$$

The first term is due to the radial variation of the tidal amplitude. The second term combines the optical and forced libration. The amplitude of the optical libration is approximately $2e$; F is the amplitude of the forced libration. The sum of the optical and radial terms gives equation (25). The third term is due to the forced secondary libration, presuming the system is in the secondary resonance. The amplitude of the forced secondary libration is approximately

$$S = 2\left(\frac{\epsilon - 1/3}{\epsilon}\right)^{1/2}. \quad (46)$$

The 3:1 secondary resonance is only present for $\epsilon > \frac{1}{3}$. The last term in equation (45) gives the heating due to satellite obliquity.

The energy dissipated in Enceladus as a function of the out-of-roundness parameter ϵ is shown in Figure 4. For this plot we assume a rigidity appropriate for ice of 4×10^{11} dyn cm^{-2}, $Q = 20$, a density of $\rho = 1.12$ g cm^{-3}, $R = 249.35$ km, and $e = 0.0045$, and we neglect the forced libration and any obliquity.

5. PLACEMENT INTO SECONDARY RESONANCE

We see that the tidal heating in Enceladus can be enhanced by 2 to 3 orders of magnitude, depending on physical parameters, over previous estimates if the rotation is in the 3:1 secondary resonance. Here we discuss some possibilities for placing Enceladus in the secondary resonance.
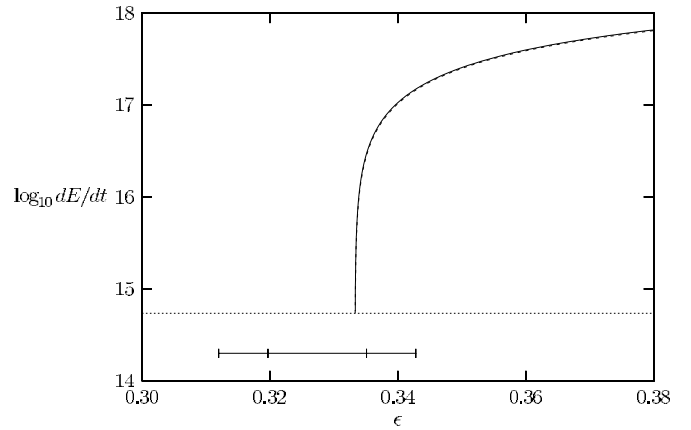

Fig. 4.—Rate of energy dissipation (ergs s^{-1}) in Enceladus in the 3:1 synchronous secondary resonance. The curves mark the dissipation using the amplitude determined numerically (*solid curve*) and using the approximate perturbative expression (*dashed curve*). The dotted horizontal line indicates the dissipation in Enceladus without the secondary resonance. The bars at the bottom indicate the range of ϵ formally allowed by the triaxial ellipsoid fit to the *Voyager* images. The inner range is 1 σ; the outer is 2 σ.

The shape of Enceladus is approximately hydrostatic (Dermott & Thomas 1994). If a hydrostatic shape is maintained as Enceladus tidally evolves away from Saturn, then there will be a corresponding change in ϵ. So tidal evolution, with hydrostatic shape, can drive the system across the secondary resonance. Unfortunately, normal tidal evolution is away from the planet, and so the shape would evolve from more out of round to less out of round (larger ϵ to smaller). This is the wrong direction for capture into the secondary resonance to occur.

Peale & Lee (2002) have recently examined scenarios for the capture of the Galilean satellite system into the Laplace resonance that involve contracting orbits. The starting point for their deliberations is the Canup & Ward (2002) model for the formation of the Galilean satellites. In this model the Galilean satellites form slowly at large radii from material streaming through the Lagrange points and spiraling onto Jupiter. The inward migration assumed by Peale & Lee results from interaction of the satellites with this same material. A similar scenario for Enceladus would provide the inward evolution that is required for Enceladus to be captured into the secondary resonance, if the inward evolution were slow enough that the shape of Enceladus remained approximately hydrostatic. Capture into the secondary resonance would have to have occurred after the orbital resonance with Dione was established, because the strength of the secondary resonance depends on the orbital eccentricity. In this scenario, Enceladus would have been in the secondary resonance for most of the age of the solar system. Why then would the resurfacing of Enceladus be episodic? Though there is considerable uncertainty, with recent estimates of cratering rates on the Saturnian satellites it is estimated that there is a nonnegligible probability that Enceladus has suffered a disruptive impact (Lissauer et al. 1988; Zahnle et al. 2003). Could Enceladus have avoided smaller impacts that might have knocked the system out of the secondary resonance?

The fact that the shape of Enceladus is nearly hydrostatic is interesting. Weisskopf (1985) argued that there is a characteristic radius, on the order of 300 km for a rocky body, below which the body should be significantly out of round, and above which the body should be nearly spherical. The argument uses

an order-of-magnitude estimate of the energy of plastic deformation. The result is roughly consistent with an observed transition to irregular shape below a radius of about 200 km among the natural satellites (Thomas et al. 1986). However, an order-of-magnitude estimate for the timescale for relaxation of an ellipsoidal distortion is $\tau = 6\eta/(\rho g R)$, where η is the viscosity, ρ is the density, g is the surface gravity, and R is the radius (Schubert et al. 2001). The viscosity depends very strongly on temperature T: using the expression for viscosity given by Schubert et al. (1986), the relaxation timescale varies from 10^{18} yr for $T = 100$ K to 10^{6} yr for $T = 200$ K. Because Enceladus is small, it is expected to be cold ($T < 100$ K) for most of its history (Ellsworth & Schubert 1983). The observed hydrostatic shape must have been achieved during formation, when the required temperature could have been reached by accretional heating, or during some later special heating episode, such as tidal heating during resonance encounter. The scenarios that involve gradual hydrostatic shape change with tidal evolution appear unlikely.

Could an impact have knocked Enceladus into the secondary resonance? Consider the case $\epsilon = 0.336$ illustrated in Figure 2. The angular velocity difference between the center of the synchronous island and the secondary resonance is about 5%. The orbital velocity of Enceladus is about 12.6 km s^{-1}; a parabolic impactor (with respect to the planet) has a velocity at the orbit of Enceladus of about 17.9 km s^{-1}. In the model of Zahnle et al. (2003), the typical impact velocity on Enceladus from ecliptic comets is 24 km s^{-1}. But if the orbits are aligned the impact velocity could be as little as 5.3 km s^{-1}. For an ideal (but unrealistic) grazing collision that imparts all its momentum to the rotation, these impact velocities imply an impactor (with density 1 g cm^{-3}) with radius in the range 6 km (for 24 km s^{-1} impact velocity) to 11 km (for 5 km s^{-1} impact velocity). For a typical 45° incidence angle these impactor radii are increased to 7 and 12 km, respectively. These impacts would produce large craters, with diameters on the order of 225 and 175 km, respectively, using the crater scaling of Zahnle et al. (2003). To give an adequate kick at smaller velocity requires a larger impactor, but as the energy scales with the square of the velocity, the larger slower impactor can leave a smaller crater. These craters would have to be in an unimaged region of Enceladus or erased by the resurfacing (and not in one of the old, heavily cratered regions). Actually, if there are large craters on Enceladus they are more likely to be found on the unimaged leading hemisphere, as the leading hemisphere is typically more heavily cratered by heliocentric comets than is the trailing hemisphere (L. Dones 2003, private communication). Using the estimated ecliptic comet cratering rates on Enceladus from Zahnle et al., Enceladus has probably only suffered a few impacts in this size range. It would be fortuitous for one of these few impactors to have hit Enceladus in just the right way to knock it into the secondary resonance. Of course, there is considerable uncertainty in the estimate of cratering populations and rates. We mention that if the impactor changes the angular momentum of Enceladus too much, then there is a possibility that the system is captured into the secondary resonance as the libration amplitude damps. However, no definitive estimate of the capture probability can be made, because it depends strongly on the tidal model.

Another possibility is that Enceladus could have suffered a number of impacts from planetocentric debris. Zahnle et al. argue that most of the impacts on Mimas are from planetocentric debris ejected from the impact that created Herschel. There are about 70 craters on Mimas with diameter larger than 20 km; they estimate that 30–100 craters in this size range would form on Mimas from Herschel ejecta. Perhaps a disruption event of some former satellite near Enceladus placed numerous multikilometer-sized objects in Enceladus-crossing orbits. The timescale for Enceladus to despin to synchronous rotation is about 60,000 yr, for $Q = 100$ (Peale 1977). As long as significant debris is swept up on shorter timescales, the spin rate and obliquity of Enceladus would evolve stochastically (Dones & Thomas 1993). The secondary resonance might then be reached by a multiple-impact process. The heavily cratered regions of Enceladus might be due to the large number of impacts of smaller debris, as is argued to be the case for Mimas. Though detailed modeling might allow a stronger case to be made for the plausibility of this scenario, there are so many possibilities and physical uncertainties that such modeling would be of questionable value. An advantage of this scenario is that Enceladus need not have or once have had a large crater.

An advantage of the impact scenarios is that they might allow for multiple resurfacings. Indeed, the rate of tidal dissipation in the secondary resonance depends primarily on the out-of-roundness parameter ϵ, and only weakly on the orbital eccentricity. An interesting possibility is that after Enceladus is placed in the secondary resonance by an impact or multiple impacts, the eccentricity decays because of the large tidal dissipation. This would cause Enceladus to temporarily retreat from the Enceladus-Dione resonance. Once the eccentricity had decayed sufficiently, the secondary resonance, whose strength depends on the eccentricity, might become unstable. Enceladus would then tidally evolve outward into the Dione resonance, reestablishing its eccentricity and, so, effectively resetting the trap until another impact again takes the system into secondary resonance.

There are other possibilities. We have only considered the simplest dynamical model here. More complete models might exhibit a richer dynamical structure. For instance, if additional perturbations broadened the 3 : 1 secondary resonance separatrix into a chaotic zone, it might be possible to evolve into this chaotic zone or the vicinity of the secondary resonance without appealing to impacts or reverse tidal evolution. And if the structure is rich enough, there might be multiple intervals of chaotic evolution, as we observed in our studies of the tidal evolution of the orbits of the Uranian satellites (Tittemore & Wisdom 1988, 1989, 1990). But these possibilities must await further study.

Consider the following scenario: Perhaps at some point Enceladus developed a figure that was more axisymmetric than hydrostatic, perhaps as the result of an impact or nonsynchronous reaccretion after a disruption event. Tidal evolution (perhaps assisted by a resonance lock with Janus, perhaps just due to Saturn tides) then established the orbital resonance lock with Dione. The resulting forced eccentricity might then provide tidal heating to raise the internal temperature of Enceladus to the point at which the relaxation time for the figure of Enceladus is short compared with the age of the solar system (only a few million years if 200 K is reached). As the figure relaxed to the observed near-hydrostatic ellipsoidal shape, the system could pass through the secondary resonance in the correct direction for capture to occur. As the resonance with Dione has already been established, the eccentricity is forced, so the secondary resonance is strong. So Enceladus would naturally evolve into the secondary resonance.

Is Enceladus currently in the secondary spin-orbit resonance? The presence of the E ring, with its short lifetime,

suggests that it might be. The Dermott & Thomas (1994) analysis of the *Voyager* data presumed exact synchronous rotation. Perhaps a less restrictive reanalysis of the *Voyager* data could place limits on the amplitude of the forced secondary libration, but new data from *Cassini* should answer this question. Even if Enceladus is not currently in the secondary resonance, the observed features might still be explained if Enceladus was recently in the resonance.

6. CONCLUSION

Enceladus is a puzzle. It shows evidence of recent resurfacing, yet the standard estimates of tidal heating, the only viable source of heating, are too small to account for the observed activity. Mimas does not show evidence of internal heating, yet the corresponding estimates of tidal heating in Mimas are 25 times larger than for Enceladus. So something must be special about Enceladus. One of the main goals of this paper is to point out that there *is* something special about Enceladus: the moments of inertia of Enceladus happen to have the right values so that the frequency of small-amplitude libration in the synchronous resonance is approximately one-third the orbital frequency. As a consequence there is a period-three bifurcation, and a chain of three secondary islands appears on the surface of section. We have developed a perturbative model for this secondary resonance. We have calculated the rate of tidal dissipation presuming Enceladus is locked in this secondary resonance and find that it can be 2 to 3 orders of magnitude larger than given by the usual tidal heating mechanism for a body in synchronous rotation. We have discussed a number of possibilities for placing Enceladus in this secondary resonance. Many of these possibilities require further study. Perhaps the most appealing involves the relaxation of an initially more axisymmetric Enceladus toward a hydrostatic shape and consequent capture into the secondary resonance. The fact that this resonance is unique to Enceladus, that significant enhancement of tidal heating would result, and that Enceladus appears to have some significant previously unexplained additional source of heating suggests that this secondary resonance is part of the explanation of the mystery of Enceladus.

REFERENCES

Canup, R. M., & Ward, W. R. 2002, AJ, 124, 3404
Dermott, S. F., & Thomas, P. C. 1988, Icarus, 73, 25
———. 1994, Icarus, 109, 241
Dones, L., & Tremaine, S. 1993, Science, 259, 350
Ellsworth, K., & Schubert, G. 1983, Icarus, 54, 490
Love, A. E. H. 1944, A Treatise on the Mathematical Theory of Elasticity (New York: Dover)
Lissauer, J. J., Peale, S. J., & Cuzzi, J. N. 1984, Icarus, 58, 159
Lissauer, J. J., Squyres, S. W., & Hartmann, W. K. 1988, J. Geophys. Res., 93, 13776
Morrison, D., Owen, T., & Soderblom, L. A. 1986, in Satellites, ed. J. A. Burns & M. S. Matthews (Tucson: Univ. Arizona Press), 764
Peale, S. J. 1977, in Planetary Satellites, ed. J. A. Burns (Tucson: Univ. Arizona Press), 87
———. 1999, ARA&A, 37, 533
———. 2003, Celest. Mech. Dyn. Astron., 87, 129
Peale, S. J., & Cassen, P. 1978, Icarus, 36, 245
Peale, S. J., Cassen, P., & Reynolds, R. T. 1979, Science, 203, 892
Peale, S. J., & Lee, M. H. 2002, Science, 298, 593
Ross, M. N., & Schubert, G. 1989, Icarus, 78, 90
Schubert, G., Spohn, T., & Reynolds, R. T. 1986, in Satellites, ed. J. A. Burns & M. S. Matthews (Tucson: Univ. Arizona Press), 224

Schubert, G., Turcotte, D. L., & Olsen, P. 2001, Mantle Convection in the Earth and Planets (Cambridge: Cambridge Univ. Press)
Squyres, S. W., & Croft, S. K. 1986, in Satellites, ed. J. A. Burns & M. S. Matthews (Tucson: Univ. Arizona Press), 293
Squyres, S. W., Reynolds, R. T., Cassen, P. M., & Peale, S. J. 1983, Icarus, 53, 319
Sussman, G. J., & Wisdom, J. 2001, Structure and Interpretation of Classical Mechanics (Cambridge: MIT Press)
Thomas, P., Veverka, J., & Dermott, S. 1986, in Satellites, ed. J. A. Burns & M. S. Matthews (Tucson: Univ. Arizona Press), 802
Thompson, W. 1863, Phil. Trans. R. Soc. London, 153, 573
Tittemore, W. C., & Wisdom, J. 1988, Icarus, 74, 172
———. 1989, Icarus, 78, 63
———. 1990, Icarus, 85, 394
Weisskopf, V. F. 1985, Am. J. Phys., 53, 19
Williams, J. G., Boggs, D. H., Ratcliff, J. T., & Dickey, J. O. 2003, in Lunar and Planetary Science XXXIV (Houston: Lunar Planet. Inst.), No. 1161
Wisdom, J. 1987, AJ, 94, 1350
Wisdom, J., Peale, S. J., & Mignard, F. 1984, Icarus, 58, 137
Zahnle, K., Schenk, P., Levison, H., & Dones, L. 2003, Icarus, 163, 263